Effect of PEDOT:PSS–molecule interface on the charge transport characteristics of the large-area molecular electronic junctions

Gunuk Wang [a], Seok-In Na [b], Tae-Wook Kim [b], Yonghun Kim [a], Sungjun Park [a], Takhee Lee [c,*]

[a] School of Materials Science and Engineering, Gwangju Institute of Science and Technology, Gwangju 500-712, Republic of Korea
[b] Institute of Advanced Composite Materials, Korea Institute of Science and Technology, Jeollabuk-do 565-902, Republic of Korea
[c] Department of Physics and Astronomy, Seoul National University, Seoul 151-747, Republic of Korea

ARTICLE INFO

ABSTRACT

We have studied the effect of the PEDOT:PSS–molecule contact on the electrical characteristics of molecular junctions consisting of N-alkanedithiol and naphthalenethiol molecules. In this study, we experimentally investigated the properties of PEDOT:PSS-interlayer molecular junctions as they depended on the two kinds of PEDOT:PSS films (the pure PEDOT:PSS film and the dimethyl sulfoxide (DMSO)-modified PEDOT:PSS film) and their thermal annealing treatment. We observed that the electrical properties of these molecular junctions are influenced by the morphology and conductivity of the PEDOT:PSS films and by the thermal treatment. In particular, the resistance of the PEDOT:PSS-interlayer molecular junctions depended on the kind of PEDOT:PSS film and the temperature, within the range of elevated temperatures (higher than room temperature) tested. These experimental results are explained by the change of the interfacial properties of the PEDOT:PSS–molecule contact, which are influenced by the morphology change of the PEDOT:PSS film and the removal of residual DMSO or water from the interface.

© 2012 Elsevier B.V. All rights reserved.

1. Introduction

Molecular electronics have attracted attention in both the scientific and industrial communities because they offer a promising route to the miniaturization of future electronic devices [1–6]. Over the past decade, considerable progress has been made in experimental methods for the study of the intrinsic charge transport characteristics through molecular layers in metal–molecule–metal junctions [7–13], and reproducible molecular electronic devices have been realized [8,10–13]. In particular, device fabrication using the conductive polymer PEDOT:PSS (poly-(3,4-ethylenedioxythiophene) stabilized with poly-(4-styrenesulphonic acid)) as a protecting interlayer between the top metal (typically Au) electrode and the self-assembled monolayer (SAM) molecules has been the subject of increased attention as a platform for stable solid-state molecular devices [8,14]. The technique based on these PEDOT:PSS-interlayer molecular junctions has several advantages. In particular, it produces reliable and reproducible molecular junctions with a very high device yield (>90%). For this reason, PEDOT:PSS-interlayer molecular junctions have been used to successfully investigate the electronic transport properties of various molecules, such as alkyl [8,14,15] and conjugated molecules [15,16]. In addition, specific electronic functionalities, such as memory [17] and photo-switching [18] have also been demonstrated with this method.

In comparison to these experimental achievements, however, few efforts have been made to understand the interface properties of the PEDOT:PSS–molecule contact in this junction technique. In fact, it is expected that the interface property of the PEDOT:PSS–molecule contact is one of the most important factors that needs to be studied to understand the charge transport characteristics of these junctions. There are several distinct features in the PEDOT:PSS-interlayer molecular junction. The resistance of the PEDOT:PSS-

* Corresponding author. Tel.: +82 2 880 4269; fax: +82 2 884 3002.
  E-mail address: tlee@snu.ac.kr (T. Lee).

interlayer molecular junction is significantly different from that of a conventional metal–molecule–metal junction that does not have a PEDOT:PSS interlayer [13,19,20]. It has been observed that the resistance of the PEDOT:PSS-interlayer molecular junction is temperature-dependent above 323 K [21]. Furthermore, the conductance for short alkanethiols (number of carbon atoms <12) was indistinguishable from that of other short molecules, and it was even indistinguishable from the case of a PEDOT:PSS-only junction [14,15]. However, the conductance of these short alkanethiol molecules can be distinguished when a different PEDOT:PSS is used in the molecular junctions [8]. These features may be fully understood in terms of the properties of the interface between PEDOT:PSS and molecules.

Here, we report our study of PEDOT:PSS-interlayer molecular junctions, focusing on the interfacial properties of the PEDOT:PSS–molecule contact. Specifically, we studied the influence of additional solvent (dimethyl sulfoxide, abbreviated as DMSO) and thermal treatment on the charge transport characteristics of the PEDOT:PSS-interlayer molecular junctions consisting of alkanedithiol and naphthalenethiol molecules. We investigated the differences in conductivity, work function, morphology, and phase image of DMSO-modified PEDOT:PSS and unmodified PEDOT:PSS by various analytic tools, such as four-point-probe, Kelvin probe, and atomic force microscope (AFM) measurements. We also developed a comprehensive explanation for the transport properties, including the resistance and the transition voltage that were influenced by the morphology of the PEDOT:PSS film and the effects of thermal annealing.

2. Experimental

2.1. Device fabrication

The junction technique in this study involves an insulating photoresist (PR) layer on the patterned (Au/Ti) bottom electrodes on a SiO_2/Si substrate to electrically isolate the molecular junctions. Holes in the photoresist layer were square-shaped with side lengths of 40 and 90 μm. After SAM formation on the bottom electrode, two types of PEDOT:PSS (a pure PH510 or a 7% DMSO-modified PH510) films were prepared by spin-coating on top of the SAMs, covering the complete devices. The thickness of the PEDOT:PSS layer was typically 200–300 nm, effectively preventing the formation of electrical shorts upon subsequent deposition of the Au top electrode. Then the Au top electrode (thickness 50–100 nm) was deposited on top of the PEDOT:PSS layer using an electron beam evaporator through a shadow mask. Reactive ion etching (RIE) with O_2 was used to remove the redundant PEDOT:PSS. The Au top electrode was used as a contact with the probes and as a shadow mask, while the PEDOT:PSS was etched away using RIE to prevent a direct current path through the PEDOT:PSS from the top electrode to the bottom electrode.

### 2.2. Formation of self-assembled monolayer

Four molecular species (DC8, DC12, DC16, and Naph-SH, Fig. 1(c) were self-assembled on the Au bottom electrodes.

For molecular deposition, we used at least 5 mM molecular solutions for an incubation time of 1–2 days in a nitrogen-filled glove box with an oxygen level of less than ∼10 ppm to avoid potential oxidation problems.

3. Results and discussion

Fig. 1 shows the schematic and the transmission electron microscopy (TEM) image of a fabricated PEDOT:PSS-interlayer molecular junction. Four molecular components were used in this study. Specifically, octanedithiol (abbreviated as DC8), dodecanedithiol (DC12), and hexadecanedithiol (DC16) were used for alkanedithiols, and naphthalene-thiol (Naph-SH) was used for an oligoacene-based molecule in this study (see Fig. 1(c)). We used two kinds of PEDOT:PSS materials (from H.C. Starck) as a conducting interlayer in our molecular junctions: pure PH510 and DMSO-modified PH510 solution. The details of the device fabrication are described in Section 2.

The morphology of the PEDOT:PSS film is an important factor for understanding and interpreting the interfacial properties of PEDOT:PSS-interlayer molecular junctions. The currently accepted morphology of spin-cast PEDOT:PSS films is that of pancake-shaped conducting PEDOT-rich cores surrounded by non-conducting PSS-rich shells [22]. Using a four-point-probe measurement (Keithley 2400 current source with an HP 34420A nanovoltmeter), the conductivity of a 7% DMSO-modified PEDOT:PSS film was observed to be, on average, ∼300 S cm^{-1} at room temperature, which is approximately three orders of magnitude greater than that observed in the case of pure PEDOT:PSS (<0.2 S cm^{-1}, 0% DMSO-modified PEDOT:PSS film) (see Fig. S1 in Supplementary data). It is well known that when DMSO is added to PEDOT:PSS, its conductivity can be improved by 2–3 orders of magnitude because of the morphological change caused by the reduction of the insulating PSS elements [23–25]. In other words, the conductivity of PEDOT:PSS is highly correlated with the total area of PEDOT-rich cores in a given unit volume or area. Fig. 2(a) show the topography and phase images of the two types of PEDOT:PSS films (pure PEDOT:PSS and 7% DMSO-modified PEDOT:PSS) obtained using an AFM (Park Systems XE-100). The average size of the PEDOT:PSS particles and their surface roughness increased with additional DMSO, leading to a better conductivity of the PEDOT:PSS film (see Fig. 2(a) and Fig. S1 in Supplementary data). The grain ratios of the PEDOT-rich cores and PSS-rich shells in the PEDOT:PSS films can be determined from their phase images [23–26]. The bright (positive degree in phase) and dark (negative degree in phase) regions in the AFM phase images correspond to the PEDOT-rich cores and the PSS-rich shells, respectively [25,26]. With DMSO added, the bright regions indicating the PEDOT:PSS-rich cores increased in area, and the dark regions corresponding to PSS-rich shells decreased accordingly (see Fig. S2 in Supplementary data). Furthermore, the phase separation between the PEDOT-rich cores and PSS-rich shells was more distinct in the 7% DMSO-modified PEDOT:PSS film than in the case of the pure PEDOT:PSS film (Fig. 2(a)). These results indicate that the 7% DMSO-modified
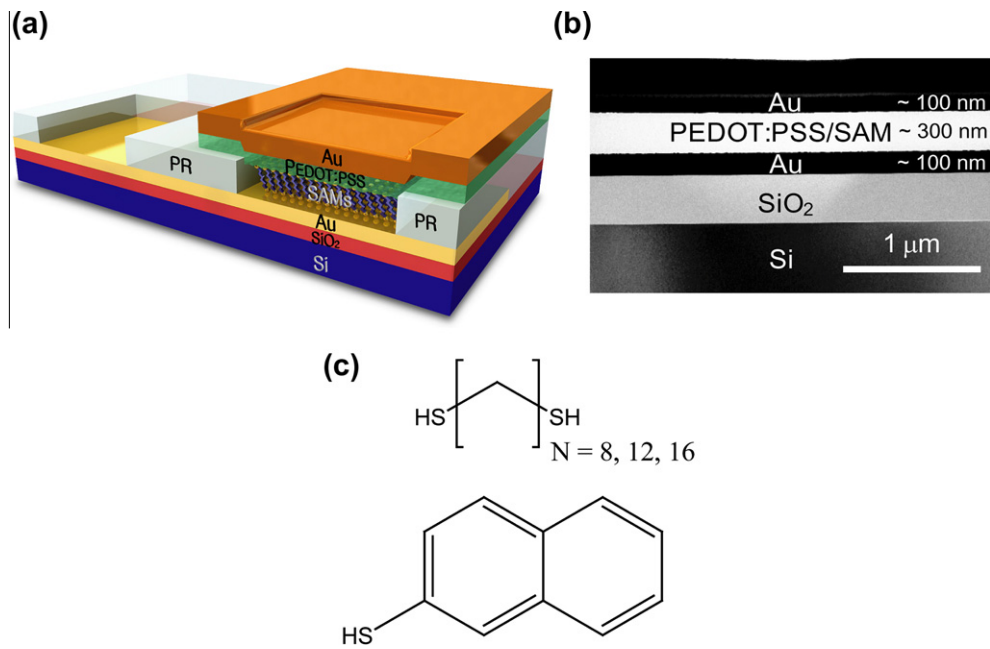
Fig. 1. (a) Schematic illustration of a PEDOT:PSS-interlayer molecular junction. (b) The cross-sectional TEM image in the active region for a molecular device. (c) The N-alkanedithiols and naphthalenethiol molecular structures are shown.
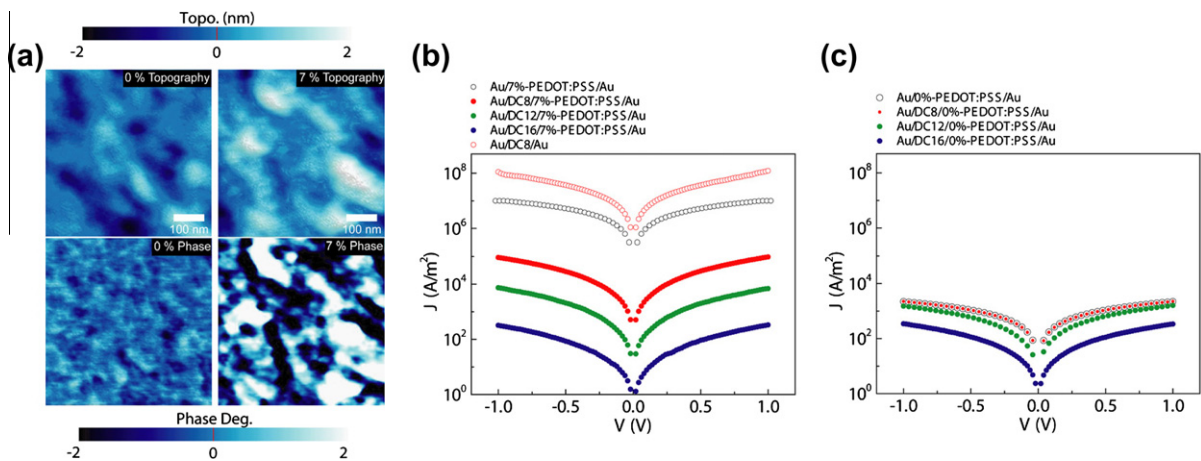
Fig. 2. (a) The AFM topography (top) and phase (bottom) images of $500 \times 500 \ nm^2$ regions of pure PEDOT:PSS and 7% DMSO-modified PEDOT:PSS films at 303 K. (b) The $J–V$ data for 7% DMSO-modified PEDOT:PSS-interlayer molecular junctions (DC8, DC12, and DC16), and Au/DC8/Au junction, and Au/7% DMSO-modified PEDOT:PSS/Au junctions at 303 K. (c) The $J–V$ data for 0% DMSO-modified PEDOT:PSS-interlayer molecular junctions (DC8, DC12, and DC16) and Au/0% DMSO-modified PEDOT:PSS/Au junctions at 303 K.

PEDOT:PSS film has larger conducting areas and thus improved conductivity as a result of the proliferation of the conducting PEDOT-rich core.

The morphology and conductivity of the PEDOT:PSS films lead to distinct features of the PEDOT:PSS-interlayer molecular junctions in comparison with conventional metal–molecule–metal junctions that do not contain a PEDOT:PSS interlayer. For example, it is difficult to investigate and distinguish the electrical properties for short molecules (such as DC8, DC12, and Naph-S) in PEDOT:PSS-interlayer molecular junctions when pure PED-

OT:PSS is used because of the low conductivity of the pure PEDOT:PSS film (Fig. 2(c) and see Fig. S5 in Supplementary data). However, for the PEDOT:PSS-interlayer molecular junctions made with 7% DMSO-modified PEDOT:PSS film, it is possible to measure and distinguish the electronic properties of short alkanedithiol molecules ($N = 8$ and 12) and conjugate Naph-S molecules because the conductance of the 7% PEDOT:PSS-only junction (without molecules) is much higher than that of the PEDOT:PSS-interlayer junction that contains molecules (Fig. 2(b) and see Fig. S5 in Supplementary data). These differences are clearly visible

in Fig. 2(a) and (b); when pure PEDOT:PSS was used, any conductance higher than the "0%-PEDOT:PSS" curve was not measurable.

It should also be noted that there is a significant discrepancy in the conductance between the Au/DC8/Au (open red[1] circles) and Au/DC8/7% PEDOT:PSS (solid red circles) molecular junctions in Fig. 2(b). Note that the J–V data for Au/DC8/Au molecular junction was reported in our previous study [9]. This conductance discrepancy can be explained by the morphological properties of the PEDOT:PSS film and the nature of contact at the interface between the PEDOT:PSS and the molecules. It has been recognized that electronic conduction through the PEDOT:PSS film takes place mainly in the PEDOT-rich core grains via hopping of charge carriers between PEDOT rich grains, not non-conducting PSS shell regions [23]. Therefore, the tunneling current through the interface between the molecules and the PEDOT-rich core is higher than that through the molecules and the PSS-rich shell. In other words, overall charge transport in the molecular junction will be more limited in the interface of molecules/PSS-rich shell regions because of the additional tunneling regions of the insulating PSS-rich shells. Therefore, the limited transport pathways produced by the insulating PSS-rich shells reduce the conductance of the molecular junctions. The different nature of the contact between S–Au and SH/PEDOT:PSS is also an important reason for the conductance discrepancy between the Au/DC8/Au and Au/DC8/PEDOT:PSS molecular junctions [19,20]. In particular, the top contact of the Au/DC8/Au junction forms a chemisorbed contact [S–Au], whereas the Au/DC8/PEDOT:PSS junction forms a physisorbed contact [SH/PEDOT:PSS] [19,20]. It is well known that chemisorbed contacts in molecular junctions have higher conductance than physisorbed contacts because of the reduced charge decay through the chemisorbed contact barrier by strong molecular overlap [9,27–29].

Another distinct feature of PEDOT:PSS-interlayer molecular junctions is the temperature (T)-dependent transport behavior at high temperatures ($T \geqslant 323$ K) [21]. Fig. 3 shows the resistances R for 7% DMSO-modified PEDOT:PSS-interlayer junctions containing alkanedithiols (DC8, DC12, and DC16) measured at different temperatures (78–383 K). Here, the resistance R was obtained from the linear fit of the J–V data in the low-bias region ($-0.1 \leqslant V \leqslant 0.1$ V). The error bar was determined from the standard deviation of the individual measurements for ∼50 different junctions. Note that the resistance of 7% PEDOT:PSS-only junction is a few order of magnitude lower than that of PEDOT:PSS-interlayer molecular junctions at the whole range of temperatures (323–383 K) (Fig. S7 in Supplementary data). A key finding in Fig. 3 is that the resistance of the molecular junctions decreased as the temperature increased (from 303 to 383 K). We note that the change of J–V curves as temperature change was irreversible (see Fig. S8 in Supplementary data). Therefore, we interpret that the irreversible J–V behavior at elevated temperature cannot be explained by the thermionic emission transport mechanism [30] or by
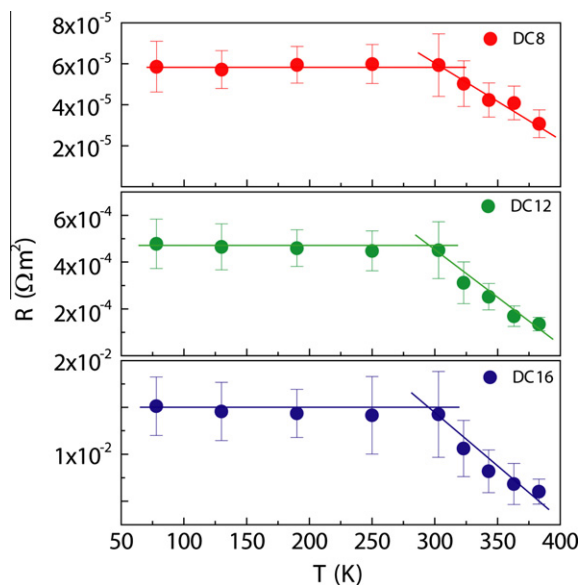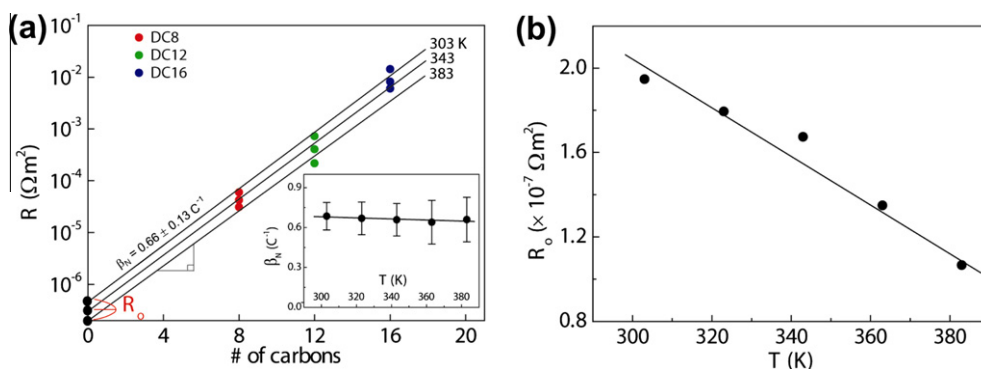

Fig. 3. A plot of resistance R versus the annealing temperature (78–383 K) for 7% DMSO-modified PEDOT:PSS-interlayer molecular junctions of DC8, DC12, and DC16 molecules.

the temperature dependence of the contact electrode's Fermi function [31,32]. The temperature-independent transport parameters (J and R) were observed when measured at temperatures lower than room temperature (from 78 to 303 K), which manifests off-resonant tunneling through the molecular barrier in this temperature range. Akkerman et al. have suggested that the decrease in the resistance R as the temperature increases is caused by the phase change of the SAM by molecular desorption or removal of the remaining water from the hydrophilic PEDOT:PSS–molecule interface [21]. However, it is difficult to directly demonstrate and analyze the nature of the phase change of the SAM in the completed PEDOT:PSS-interlayer junction.

To better understand the physical or chemical causes for the temperature-dependent transport behaviors in PEDOT:PSS-interlayer molecular junctions, we measured and determined various parameters such as the decay coefficients β_N, the contact resistances R_o, and the transition voltages V_T of the junctions, as well as the phase image, conductivity, and grain size of the PEDOT:PSS films as a function of temperature. These results are summarized in Figs. 4–6. Fig. 4(a) shows the resistance, R, as a function of the number of carbons (N = 8, 12, and 16) in the molecules and the temperature of thermal annealing (T = 303, 343, and 383 K) that was performed on the alkanedithiol PEDOT–PSS interlayer molecular junctions. The value of R increases exponentially with the number of carbons in the molecule, following the typical tunneling equation of $R = R_o \exp(\beta_N N)$ [7–9]. R_o is an effective contact resistance that depends on the molecule/electrode contact, and β_N is a decay coefficient that depends on the molecular structure, which can be obtained by taking the linear fit of a logarithmic R–N plot [28]. β_N reflects the degree to which the wave function decreases for the tunneling charge [29]. The observed β_N value at 303 K was 0.69 ± 0.10 C^{-1}, which is

---

[1] For interpretation of color in Fig. 2, the reader is referred to the web version of this article.

Fig. 4. (a) A plot of resistance R versus the number of molecular carbons of DC8, DC12, and DC16 PEDOT:PSS-interlayer molecular junctions. The solid lines are the exponential fitting results, which give β_N as a function of the annealing temperature (inset). The y-intercept points are the effective contact resistance R_o. (b) A plot of R_o versus the annealing temperatures.
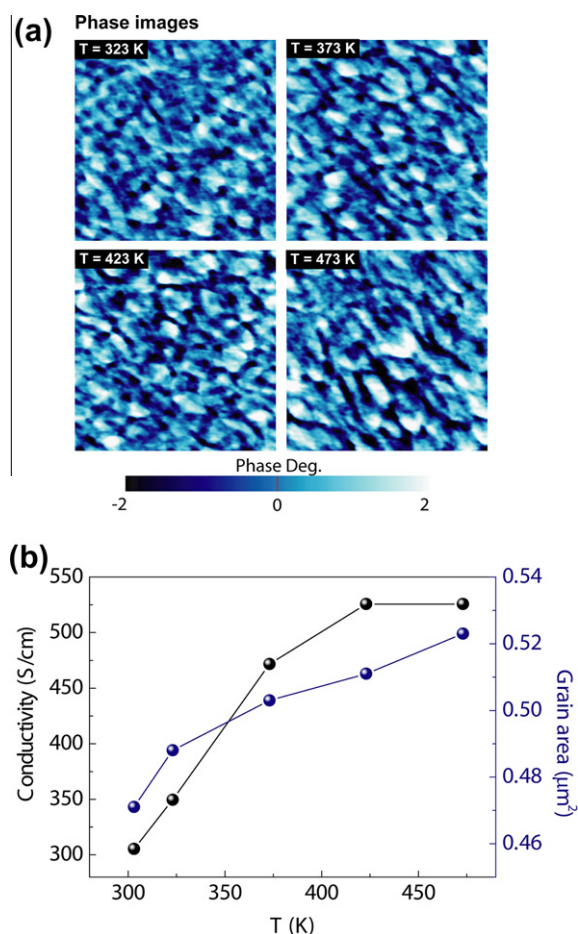

Fig. 5. (a) The AFM phase images of $1 \times 1\ \mu m^2$ regions of 7% DMSO-modified PEDOT:PSS films at different annealing temperatures (323–473 K, step 50 K). (b) Temperature dependence of conductivity and grain area for 7% DMSO-modified PEDOT:PSS films.

consistent with previously reported values for PEDOT:PSS-interlayer molecular junctions [8,33].

Interestingly, similar β_N values were observed regardless of the annealing temperatures (Fig. 4(a) and the inset).

This result indicates that the tunneling efficiency through the molecular structure was maintained, regardless of any thermal annealing effect. In other words, there was no significant change in the structure and phase of the SAM itself in the molecular junctions at elevated temperature. However, the effective contact resistance R_o in the molecular junctions, which is defined as the resistance extrapolated at the number of carbons $N = 0$, was found to linearly decrease as the temperature increased, as shown in Fig. 4(b). Therefore, it is reasonable to postulate that the change of the properties of the interface between PEDOT:PSS and the SAM with changing temperature is the main cause for the reduction of the contact resistance in the PEDOT–PSS interlayer molecular junctions, but not the phase change of the SAM itself.

The change in the conductivity of an annealed PEDOT:PSS film is strongly related to the thermally-induced morphological change of the film [21,34,36]. In the case of the DMSO-modified PEDOT:PSS film, the morphological change continues until the additional DMSO (or residual water) is entirely evaporated [24–26,35]. We also confirmed that thermal annealing removes DMSO from our 7% DMSO-modified PEDOT:PSS film using proton nuclear magnetic resonance (H-NMR) (JEOL JNR-LA300WB 30 MHz) measurements (Fig. S4 in Supplementary data). Fig. 5(a) shows AFM phase images of the 7% DMSO- modified PEDOT:PSS film annealed at different temperatures (323, 373, 423, and 473 K). The images in this Fig. 5(a) were obtained after the film was annealed at different temperatures and then cooled to room temperature. Fig. 5(b) shows the correlation between the conductivity and the grain size of the PEDOT-rich cores in the 7% DMSO-modified PEDOT:PSS film for different annealing temperatures. Note that the grain size of the PEDOT-rich cores (positive degree in phase) was calculated from XEI software (Park Systems XE-100) (Fig. S3 in Supplementary data). The bright region (PEDOT-rich cores) in the 7% DMSO-modified PEDOT:PSS film increased as the temperature increased, which resulted in the enhancement of the conductivity of the film. Therefore, we can say that the thermal treatment on the PEDOT:PSS film had two effects on the molecular junctions: (i) the grain size of the PEDOT-rich cores at the SAM/
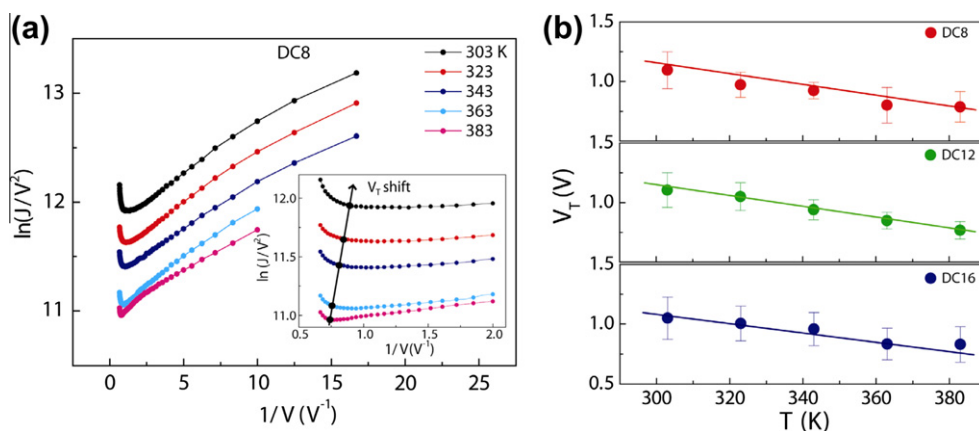
Fig. 6. (a) ln(J/V^2) versus 1/V curves for DC8 PEDOT:PSS-interlayer molecular junctions measured at different temperatures (303–383 K, 20 K step). Inset is a zoomed-in plot near the transition voltages V_T (minimum points of the curves). (b) Experimental V_T for DC8, DC12, and DC16 PEDOT:PSS-interlayer molecular junctions in the temperature range from 303 to 383 K.

PEDOT:PSS interface increased, and (ii) the remaining DMSO and water in the junctions evaporate. These two effects lead to the enhancement of conductance of the molecular junctions. It is possible that the SAM and PEDOT:PSS film can produce a better conducting contact in the junctions because of the increased grain size of the conducting PEDOT-rich cores, which leads to the reduction of the resistance of the molecular junction (see Fig. 4(b)). In addition, the residual DMSO or water at the SAM and PEDOT:PSS film can act as an additional contact barrier [36]. Therefore, desorption of DMSO or water from the interface between the SAM and the PEDOT:PSS film by thermal treatment reduces the contact resistance (see Fig. 4(a)).

The transition voltage V_T is defined as the minimum point on a plot of ln(I/V^2) versus 1/V (Fowler–Nordheim (FN) plot), which can estimate the position of the nearest orbital levels with respect to the Fermi energy of the electrodes, i.e., V_T can yield information concerning the overall tunneling barrier height in the junction [37]. Typically, the V_T value depends on the work functions of the contact electrodes [38], the orbital levels of molecule [36], the degree of asymmetric coupling [16,40,41], and any contact groups that affect the tunneling barrier height [16,38]. As mentioned above, the removal of residual DMSO or water between the SAM and the PEDOT:PSS film leads to the reduction of the contact barrier in the molecular junction. Therefore, it is expected that the V_T value of a PEDOT:PSS-interlayer molecular junction can also be influenced by thermal annealing. Fig. 6(a) shows a ln(I/V^2) versus 1/V plot measured at elevated temperatures (303–383 K, 20 K step). The minimum points in the FN plots for the DC8 junctions (shown more clearly in the inset of Fig. 6(a)) shifted to a lower voltage (specifically, from 1.10 ± 0.15 V at 303 K to 0.79 ± 0.13 at 383 K) as temperature increased. Similar behaviors were consistently observed for the other molecular systems (DC12, DC16, and Naph-SH) (Fig. 6(b) and Fig. S6 in Supplementary data). The error bars in Fig. 6(b) denote the standard deviations of the individual measurements for ~50 devices. In general, the alkanethiol molecular junctions show molecular-length-independent transition voltage V_T behavior due to the similar HOMO–LUMO gap

for different length alkanethiols, which has been demonstrated from several groups' experimental results and theories [37–39]. In other words, V_T strongly depends on the energy offset (barrier height) for the molecular junctions, but is not sensitively dependent on the molecular length for alkanethiols (particularly in case of the number of carbon $N > 6$) or tunneling length. Consequently, we think that the lowered V_T of the molecular junctions at elevated temperatures ($\geqslant$ 323 K) indicates that the effective tunneling barrier is lowered, which is related to the reduction of contact barrier at SAM/PEDOT:PSS interface by the increase of grain size of the PEDOT-rich cores and the evaporation of the remaining DMSO and water from interface. Therefore, it is reasonable to interpret that the change in the J–V curves under elevated temperature is influenced both by the lowered contact barrier height (or V_T), and by the decrease in the tunnel thickness by the removal DMSO (or water) in interface.

4. Conclusions

In summary, we experimentally investigated the effect of the PEDOT:PSS–molecule contact on the charge transport characteristics of molecular junctions consisting of alkanedithiol and naphthalenethiol molecules and the variance of those characteristics with two kinds of PEDOT:PSS films (pure PEDOT:PSS and 7% DMSO-modified PEDOT:PSS films) and thermal annealing. We demonstrated that electrical parameters, such as resistance, contact resistance, and transition voltage depended on the kind of PEDOT:PSS film and the temperature, particularly at elevated temperatures (higher than room temperature). Specifically, we found that the morphological change produced on a PEDOT:PSS film by DMSO led to conductivity enhancement. The resistance, contact resistance, and transition voltage of the PEDOT:PSS-interlayer molecular junctions decreased as the temperature increased because of the increased grain size of the PEDOT-rich cores and the removal of residual DMSO or water from the PEDOT:PSS–molecules interface. This study may enhance the understanding of

the transport characteristics of high yield PEDOT:PSS-interlayer molecular electronic devices in terms of the properties of the interface between PEDOT:PSS and molecules.

Acknowledgements

Appendix A. Supplementary data

Supplementary data associated with this article can be found, in the online version, at doi:10.1016/j.orgel.2012.02.002.

References

[1] C. Joachim, J.K. Gimzewski, A. Aviram, Nature 408 (2000) 541.
[2] M.A. Reed, C. Zhou, C.J. Muller, T.P. Burgin, J.M. Tour, Science 278 (1997) 252.
[3] J.C. Love, L.A. Estroff, J.K. Kriebel, R.G. Nuzzo, G.M. Whitesides, Chem. Rev. 105 (2005) 1103.
[4] J. Heath, M. Ratner, Phys. Today 56 (2003) 43.
[5] R.L. McCreery, A.J. Bergren, Adv. Mater. 21 (2009) 4303.
[6] L. Luo, S.H. Choi, C.D. Frisbie, Chem. Mater. 23 (2010) 631.
[7] W. Wang, T. Lee, M.A. Reed, Phys. Rev. B 68 (2003) 035416.
[8] H.B. Akkerman, P.W.M. Blom, D.M. de Leeuw, B. de Boer, Nature 441 (2006) 69.
[9] T.-W. Kim, G. Wang, H. Lee, T. Lee, Nanotechnology 18 (2007) 315204.
[10] G.S. Bang, H. Chang, J.-R. Koo, T. Lee, R.C. Advincula, H. Lee, Small 4 (2008) 399.
[11] C.A. Nijhuis, W.F. Reus, G.M. Whitesides, J. Am. Chem. Soc. 131 (2009) 17814.
[12] A.P. Bonifas, R.L. McCreery, Nat. Nanotechnol. 5 (2010) 612.
[13] G. Wang, Y. Kim, M. Choe, T.-W. Kim, T. Lee, Adv. Mater. 23 (2011) 755.
[14] P.A. Van Hal, E.C.P. Smits, T.C.T. Geuns, H.B. Akkerman, B.C. De Brito, S. Perissinotto, G. Lanzani, A.J. Kronemeijer, V. Geskin, J. Cornil, P.W.M. Blom, B. De Boer, D.M. De Leeuw, Nat. Nanotechnol. 3 (2008) 749.
[15] A.J. Kronemeijer, I. Katsouras, E.H. Huisman, P.A. van Hal, T.C.T. Geuns, P.W.M. Blom, D.M. de Leeuw, Small 7 (2011) 1593.
[16] G. Wang, Y. Kim, S.-I. Na, Y.H. Kahng, J. Ku, S. Park, Y.H. Jang, D.-Y. Kim, T. Lee, J. Phys. Chem. C 115 (2011) 17979.
[17] J. Lee, H. Chang, S. Kim, G.S. Bang, H. Lee, Angew. Chem. Int. Ed. 48 (2009) 8501.
[18] A.J. Kronemeijer, H.B. Akkerman, T. Kudernac, B.J. van Wees, B.L. Feringa, P.W.M. Blom, B. de Boer, Adv. Mater. 20 (2008) 1467.
[19] G. Wang, H. Yoo, S.-I. Na, T.-W. Kim, B. Cho, D.-Y. Kim, T. Lee, Thin Solid Films 518 (2009) 824.
[20] H.B. Akkerman, B. de Boer, J. Phys. Condens. Matter 20 (2008) 01300.
[21] H.B. Akkerman, A.J. Kronemeijer, J. Harkema, P.A. van Hal, E.C.P. Smits, D.M. de Leeuw, P.W.M. Blom, Org. Electron. 11 (2010) 146.
[22] U. Lang, E. Müller, N. Naujoks, J. Dual, Adv. Funct. Mater. 19 (2009) 1215.
[23] A.M. Nardes, R.A.J. Janssen, M. Kemerink, Adv. Funct. Mater. 18 (2008) 865.
[24] S.-I. Na, G. Wang, S.-S. Kim, T.-W. Kim, S.-H. Oh, B.-K. Yu, T. Lee, D.-Y. Kim, J. Mater. Chem. 19 (2009) 9045.
[25] Y.H. Kim, C. Sachse, M.L. Machala, C. May, L. Müller-Meskamp, K. Leo, Adv. Funct. Mater. 21 (2011) 1076.
[26] X. Crispin, F.L.E. Jakobsson, A. Crispin, P.C.M. Grim, P. Andersson, A. Volodin, C. van Haesendonck, M. Van der Auweraer, W.R. Salaneck, M. Berggren, Chem. Mater. 18 (2006) 4354.
[27] X.D. Cui, A. Primak, X. Zarate, J. Tomfohr, O.F. Sankey, A.L. Moore, T.A. Moore, D. Gust, G. Harris, S.M. Lindsay, Science 294 (2001) 571.
[28] V.B. Engelkes, J.M. Beebe, C.D. Frisbie, J. Am. Chem. Soc. 126 (2004) 14287.
[29] G. Wang, T.-W. Kim, H. Lee, T. Lee, Phys. Rev. B 76 (2007) 205320.
[30] R.L. McCreery, Chem. Mater. 16 (2004) 4477.
[31] M. Poot, E. Osorio, K. O'Neill, J.M. Thijssen, D. Vanmaekelbergh, C.A. van Walree, L.W. Jenneskens, H.S.J. van der Zant, Nano Lett. 6 (2006) 1031.
[32] A.J. Bergren, R.L. McCreery, S.R. Stoyanov, S. Gusarov, A. Kovalenko, J. Phys. Chem. C 114 (2010) 15806.
[33] G. Wang, T.-W. Kim, T. Lee, J. Mater. Chem. 21 (2011) 18097.
[34] E. Vitoratos, S. Sakkopoulos, E. Dalas, N. Paliatsas, D. Karageorgopoulos, F. Petraki, S. Kennou, S.A. Choulis, Org. Electron. 10 (2008) 1.
[35] A.M. Nardes, M. Kemerink, M.M. de Kok, E. Vinken, K. Maturova, R.A.J. Janssen, Org. Electron. 9 (2008) 727.
[36] S. Wolfgang, Surf. Sci. 335 (1995) 416.
[37] J.M. Beebe, B. Kim, J.W. Gadzuk, C. Daniel Frisbie, J.G. Kushmerick, Phys. Rev. Lett. 97 (2006) 026801.
[38] J.M. Beebe, B. Kim, C.D. Frisbie, J.G. Kushmerick, ACS Nano 2 (2008) 827.
[39] E.H. Huisman, C.M. Guédon, B.J. van Wees, S.J. van der Molen, Nano Lett. 9 (2009) 3909.
[40] N. Bennett, G. Xu, L.J. Esdaile, H.L. Anderson, J.E. Macdonald, M. Elliott, Small 6 (2010) 2604.
[41] J. Chen, T. Markussen, K.S. Thygesen, Phys. Rev. B 82 (2010) 121412.